On the Time-Delay Estimation Accuracy Limit of GNSS Meta-Signals

Lorenzo Ortega[1], Jordi Vilà-Valls[2], Eric Chaumette[2] and François Vincent[2]

***Abstract*— In standard two-step Global Navigation Satellite Systems (GNSS) receiver architectures the precision on the position, velocity and time estimates is driven by the precision on the intermediate parameters, i.e., delays and Dopplers. The estimation of the time-delay is in turn driven by the baseband signal resolution, that is, by the type of broadcasted signals. Among the different GNSS signals available the so-called AltBOC modulated signal, appearing in the Galileo E5 band and the new GNSS meta-signal concept, is the one which may provide the better time-delay precision. In order to meet the constraints of safety-critical applications such as Intelligent Transportation Systems or automated aircraft landing, it is fundamental to known the ultimate code-based precision achievable by standalone GNSS receivers. The main goal of this contribution is to assess the time-delay precision of AltBOC type signals. The analysis is performed by resorting to a new compact closed-form Cramér-Rao bound expression for time-delay estimation which only depends on the signal samples. In addition, the corresponding time-delay maximum likelihood estimate is also provided to assess the minimum signal-to-noise ratio that allows to be in optimal receiver operation.**

I. Introduction

In the context of Intelligent Transportation Systems (ITS), either for autonomous cars, ships or unmanned ground/air vehicles (robots/drones), positioning, navigation and timing (PNT) systems are a fundamental key component to design reliable, safe and smart ecosystems. More precisely, there is an actual need to provide precise, continuous and reliable navigation information, not only for the autonomous system itself but also for vulnerable road user such as cyclists and pedestrians, and upper layers of the system dealing, for instance, with traffic control and emergency services.

Several navigation systems are available, from Global Navigation Satellite Systems (GNSS), to alternative ranging strategies exploiting cellular signals (LTE/5G) or dedicated infrastructure (i.e., IR-UWB), vehicle-to-everything (V2X) communications to obtain peer-to-peer measurements, local inertial navigation systems (INS), or possible combinations of these standalone solutions. Among them, the main player and positioning gold standard source of navigation information is GNSS, both standalone or in multi-sensor data fusion strategies. But notice that these GNSS still have several limitations to be used as standalone navigation system: i) they may be affected by attacks such as jamming and spoofing [1], ii) be severely degraded in non-nominal propagation conditions [2], or iii) lack the precision needed in the ITS context (i.e., sub-meter lane-level precision). In this contribution we further explore the latter.

In the context of precise navigation, it is common practice to resort to carrier phase-based differential techniques such as Real-Time Kinematics (RTK) [3, Ch. 26], or Precise Point Positioning (PPP) techniques [3, Ch. 25]. The former require a reference station and are only valid for short baseline ranges to ensure that the two receivers observe the same propagation errors. The latter require precise satellite orbit, clocks and propagation errors corrections, and need a long convergence time of tens of minutes, which limit their use for many practical real-time applications. In both cases the main problem is the resolution of carrier phase ambiguities (i.e., unknown number of cycles inside the baseband signal resolution). On the other hand, the precision of standard code-based GNSS navigation is driven by the baseband signal resolution, that is, by the type of signal broadcasted by the satellites (i.e., Pseudo-Random Noise (PRN) codes and subcarrier modulation), which may be on the order of some meters for the most basic signals (i.e., GPS L1 C/A).

In conventional two-step GNSS receiver architectures, the positioning precision is linked to the precision on the time-delay estimation, which can be assessed by resorting to the Cramér-Rao bound (CRB) [4], an accurate lower bound on the mean square error (MSE) sense under certain conditions (i.e., in the high signal-to-noise ratio (SNR) regime). Among the different GNSS signals the ones which may provide a better time-delay precision are the so-called Alternate Binary Offset Carrier (AltBOC), used in the complete Galileo E5 band but which also appear within the context of GNSS meta-signals [5], [6], being a promising solution for code-based precise navigation. In this article, we aim to evaluate the achievable time-delay estimation performance (i.e. assuming no external errors such as atmospherics delays, orbital or satellite clock errors, or environment-specific effects) of these AltBOC and GNSS meta-signals. To provide this performance assessment we resort to a recently proposed time-delay estimation compact-form CRB expression which only depends on the signal samples [7]. This new CRB is computed for the different combinations of GNSS bands (i.e., E5A+E5B, E5A + E6-BC, E5B + E6-BC) in order to assess which is the ultimate time-delay precision achievable by a standalone GNSS receiver. These results are compared to the legacy GPS L1 C/A and standalone E6 and E5B signals. Finally, in order to validate the CRB and obtain the minimum SNR which allows an optimal receiver operation point, we also provide the corresponding time-delay maximum likelihood estimate (MLE), known to be asymptotically efficient.

[1] L. Ortega is a research engineer at TéSA Laboratory, Toulouse, France lorenzo.ortega@tesa.prd.fr

[2] J. Vilà-Valls, E. Chaumette and F. Vincent are with ISAE-SUPAERO, University of Toulouse, France. name.surname@isae-supaero.fr

Partially supported by the DGA/AID project 2019.65.0068.00.470.75.01 and the TéSA Lab Postdoctoral Research Fellowship.

II. Signal Model

We consider the transmission of a band-limited GNSS signal $c(t)$ (bandwidth B), so-called PRN code in the GNSS terminology, over a carrier frequency f_c ($\lambda_c = \frac{c}{f_c}$), from a transmitter (satellite) T at position $\mathbf{p}_T(t) = \mathbf{p}_T + \mathbf{v}_T t$ to a receiver R at position $\mathbf{p}_R(t) = \mathbf{p}_R + \mathbf{v}_R t$. The complex analytic signal at the output of the receiver's antenna can be written as $x_A(t) = \alpha_R c_R(t) + n_A(t)$, with $n_A(t)$ a zero-mean white complex Gaussian noise, and where the gain α_R depends on the transmitted signal power, the transmitter/receiver antenna gains and polarization vectors, and the radial distance between T and R, $\mathbf{p}_{TR}(t)$ [8], [9]. If this radial distance can be approximated by a first order model,

$$\|\mathbf{p}_{TR}(t)\| \triangleq \|\mathbf{p}_R(t) - \mathbf{p}_T(t - \tau(t))\| = c\tau(t) \simeq d + vt,$$

with $\tau(t) = \tau + bt$, $\tau = d/c$ and $b = v/c$. Using the standard narrow-band assumption then

$$c_R(t) = c(t - \tau) e^{-j2\pi f_c \tau} e^{j2\pi f_c (1-b)t}, \tag{1}$$

and the baseband output of the receiver's Hilbert filter is

$$x(t) = \alpha c(t - \tau) e^{-j2\pi f_c bt} + n(t), \tag{2}$$

with $n(t)$ a complex white Gaussian noise within the filter bandwidth with unknown variance σ_n^2, and $\alpha = \alpha_R e^{-j2\pi f_c \tau}$. The discrete vector signal model is build from $N = N_2 - N_1 + 1$ samples at $T_s = \frac{1}{F_s}$,

$$\begin{aligned}
\mathbf{x} &= \alpha \mathbf{a}(\boldsymbol{\eta}) + \mathbf{n}, \qquad (3)\\
\mathbf{x} &= (x(N_1 T_s), \ldots, x(N_2 T_s))^\top,\\
\mathbf{n} &= (n(N_1 T_s), \ldots, n(N_2 T_s))^\top,\\
\mathbf{c}(\tau) &= (c(N_1 T_s - \tau), \ldots, c(N_2 T_s - \tau))^\top,\\
\mathbf{a}(\boldsymbol{\eta}) &= ((\mathbf{c}(\tau))_1 e^{-j2\pi f_c b N_1 T_s}, \ldots, (\mathbf{c}(\tau))_N e^{-j2\pi f_c b N_2 T_s})^\top,
\end{aligned}$$

where $\boldsymbol{\eta} = [\tau, b]^T$, $\mathbf{n} \sim \mathcal{CN}(\mathbf{0}, \sigma_n^2 \mathbf{I}_N)$. Since the transmitter/receiver antenna gains and polarization vectors are in general unknown, α is assumed to be an unknown complex parameter as well [9]–[13]. Thus, the unknown deterministic parameters [14] can be gathered in vector $\underline{\boldsymbol{\epsilon}} = [\sigma_n^2, \tau, b, \alpha, \alpha^*]^T$, where α^* is the complex conjugate of α.

III. Time-delay CRB for Band-limited Signals and Maximum Likelihood Estimation

A. CRB for Time-delay Estimation

In a recent contribution [7] we derived a new compact closed-form CRB for the time-delay estimation of a generic band-limited signal, given by

$$\begin{aligned}
F_{\tau|\underline{\boldsymbol{\epsilon}}}(\underline{\boldsymbol{\epsilon}}) &= 2\mathrm{SNR}_{\text{out}} F_s^2 \left(\frac{\mathbf{c}^H \mathbf{V} \mathbf{c}}{\mathbf{c}^H \mathbf{c}} - \left| \frac{\mathbf{c}^H \boldsymbol{\Lambda} \mathbf{c}}{\mathbf{c}^H \mathbf{c}} \right|^2 \right)\\
&\underset{\text{real signal}}{=} 2\mathrm{SNR}_{\text{out}} F_s^2 \left(\frac{\mathbf{c}^H \mathbf{V} \mathbf{c}}{\mathbf{c}^H \mathbf{c}} \right), \qquad (4)
\end{aligned}$$

where $\mathrm{SNR}_{\text{out}} = \frac{|\alpha|^2 \mathbb{E}}{(\sigma_n^2/F_s)} = \frac{|\alpha|^2}{\sigma_n^2} \mathbf{c}^H \mathbf{c}$ and $\mathbb{E}$ the energy of the signal. $\boldsymbol{\Lambda}$ and $\mathbf{V}$ are defined as (for $N_1 \leqslant n, n' \leqslant N_2$)

$$(\mathbf{V})_{n,n'} = \begin{cases} n' \neq n : (-1)^{|n-n'|} \frac{2}{(n-n')^2} \\ n' = n : \frac{\pi^2}{3} \end{cases} \tag{5a}$$

$$(\boldsymbol{\Lambda})_{n,n'} = \begin{cases} n' \neq n : \frac{(-1)^{|n-n'|}}{(n-n')} \\ n' = n : 0 \end{cases} . \tag{5b}$$

B. Maximum Likelihood Time-delay Estimator

Considering the signal model (3), the time-delay MLE is defined as[1] [13]

$$\begin{aligned}
\hat{\tau} &= \arg\min_\tau \left\{ \mathbf{x}^H \boldsymbol{\Pi}^\perp_{\mathbf{c}(\tau)} \mathbf{x} \right\} = \arg\max_\tau \left\{ \frac{\left| \mathbf{c}(\tau)^H \mathbf{x} \right|^2}{\mathbf{c}(\tau)^H \mathbf{c}(\tau)} \right\}\\
&= \arg\max_\tau \left\{ \frac{\left| \int_{-\infty}^{+\infty} c(t - \tau)^* x(t)\, dt \right|^2}{\int_{-\infty}^{+\infty} |c(t)|^2 dt} \right\}, \qquad (6)
\end{aligned}$$

which is useful to determine the value of $\mathrm{SNR}_{\text{out}}$ (threshold) which allows to reach the CRB, because it is known that such estimator is asymptotically efficient (e.g., in the high SNR regime) for the conditional signal model of interest [15] [16].

IV. Introduction to GNSS Meta-Signals

In this section, we present the concept of *GNSS meta-signals*, introduced for the first time in [5]. The GNSS meta-signal idea is that two different GNSS signals transmitted at two different carrier frequencies can be expressed as a single Alternate Binary Offset Carrier (AltBOC) modulated signal [17]. Based on that initial work, [6] further discussed the fundamental concept of GNSS meta-signals, proving through analytical and practical implementations that unlike other conventional methods, where GNSS receivers process multiple signals, the GNSS meta-signal method was capable to improve the single-point ranging accuracy over that of the better of the two generating signals.

A. Generalized AltBOC

The AltBOC modulation was original introduced as a method to combine Galileo signals within the E5a and E5b bands. This solution was rapidly accepted by the Galileo Signal Task Force (GSTF) due to the fact that the AltBOC modulation: i) provides a Constant Envelope Modulation (CEM), which avoids non-linear distortions at the output of the High Power Amplifier (HPA), and ii) it provides a high level of isolation between two frequency bands [17].

The easiest form of AltBOC modulation is the one where two independent PRN codes are multiplexed. Let us define the BOC subcarrier with cosine and sine phasing as,

$$SC_{cos}(t) = \mathit{sign}(\cos(2\pi F_{sub} t)) , \tag{7}$$

$$SC_{sin}(t) = \mathit{sign}(\sin(2\pi F_{sub} t)) . \tag{8}$$

[1] Let $S = span(\mathbf{A})$, with $\mathbf{A}$ a matrix, be the linear span of the set of its column vectors, $S^\perp$ the orthogonal complement of the subspace S, $\boldsymbol{\Pi}_{\mathbf{A}} = \mathbf{A}(\mathbf{A}^H \mathbf{A}) \mathbf{A}^H$ the orthogonal projection over S, and $\boldsymbol{\Pi}^\perp_{\mathbf{A}} = \mathbf{I} - \boldsymbol{\Pi}_{\mathbf{A}}$.

where F_{sub} represents the subcarrier frequency. Then, we can built the Single Side Band (SSB) subcarrier SC_{SSB} and its conjugate SC^*_{SSB} as,

$$SC_{4,SSB}(t) = \frac{1}{\sqrt{2}}\left(SC_{cos}(t) + j \cdot SC_{sin}(t)\right) , \quad (9)$$

$$SC^*_{4,SSB}(t) = \frac{1}{\sqrt{2}}\left(SC_{cos}(t) - j \cdot SC_{sin}(t)\right) . \quad (10)$$

Note that (9) can take 4 values and it can be also derived as,

$$\begin{cases} SC_{SSB}(t) & = & e^{j\left(\frac{\pi}{4}+i\cdot\frac{\pi}{2}\right)}; \\ t \mod T_{sub} & \in & \left[\frac{i\cdot T_s}{4}, \frac{(i+1)\cdot T_{sub}}{4}\right], \end{cases} \quad (11)$$

with $i \in [0,1,2,3]$ and $T_{sub} = 1/F_{sub}$. Finally, the 2 code AltBOC can be defined as,

$$\begin{aligned} c(t) &= c_A(t)SC^*_{4,SSB}(t) + c_B(t)SC_{4,SSB}(t) \\ &= \left[c_A(t) + c_B(t)\right] SC_{cos}(t) \\ &+ j \cdot \left[c_B(t) - c_A(t)\right] SC_{sin}(t) \end{aligned} \quad (12)$$

where $c_A(t)$ and $c_B(t)$ represent binary PRN codes of the low (A) and high (B) band signals, respectively. Note from the previous equation that codes $c_A(t)$ and $c_B(t)$ are not required to have the same chip rate.

Considering two independent codes (in-phase/quadrature) per each frequency band, a 4 code AltBOC modulation can be expressed as,

$$\begin{aligned} c(t) &= \left[c_{A,I}(t) + j \cdot c_{A,Q}(t)\right] SC^*_{4,SSB}(t) \\ &+ \left[c_{B,I}(t) + j \cdot c_{B,Q}(t)\right] SC_{4,SSB}(t) \end{aligned} \quad (13)$$

where $c_{A,I}(t)$ and $c_{A,Q}(t)$ represent binary in-phase/quadrature codes of the A band and $c_{B,I}(t)$ and $c_{B,Q}(t)$ represent binary in-phase/quadrature codes of the B band. The resulting constellation from (13) was shown in [17] to not a have constant envelope and consequently such modulation cannot be used with HPA working at the saturation point. In order to obtain a CEM, an intermodulation product [18] must be added within the composite signal, yielding (13) to [19],

$$\begin{aligned} c(t) &= \left[c_{A,I}(t) + j \cdot c_{A,Q}(t)\right] SC^*_{8,SSB}(t) \\ &+ \left[c_{B,I}(t) + j \cdot c_{B,Q}(t)\right] SC_{8,SSB}(t) \\ &+ \left[\overline{c_{A,I}(t)} + j \cdot \overline{c_{A,Q}(t)}\right] SC^*_{P,8,SSB}(t) \\ &+ \left[\overline{c_{B,I}(t)} + j \cdot \overline{c_{B,Q}(t)}\right] SC_{P,8,SSB}(t) \end{aligned} \quad (14)$$

where,

$$\begin{aligned} \overline{c_{A,I}(t)} &= c_{A,Q}(t)c_{B,I}(t)c_{B,Q}(t), \\ \overline{c_{A,Q}(t)} &= c_{A,I}(t)c_{B,I}(t)c_{B,Q}(t), \\ \overline{c_{B,I}(t)} &= c_{B,Q}(t)c_{A,I}(t)c_{A,Q}(t), \\ \overline{c_{B,Q}(t)} &= c_{B,I}(t)c_{A,I}(t)c_{A,Q}(t), \end{aligned} \quad (15)$$

and $SC_{8,SSB}(t)$ is the SSB "single" subcarrier of the 4 code AltBOC. Moreover, $SC_{P,8,SSB}(t)$ is defined as the "product" subcarrier. Both subcarriers can take 8 different values [17],

$$\begin{cases} SC_{8,SSB}(t) & = & e^{j\left(\frac{\pi}{8}+i\cdot\frac{\pi}{4}\right)}; \\ t \mod T_{sub} & \in & \left[\frac{i\cdot T_{sub}}{8}, \frac{(i+1)\cdot T_s}{8}\right], \end{cases} \quad (16)$$

$$\begin{cases} SC_{P,8,SSB}(t) & = & e^{j\left(\frac{5\pi}{8}-i\cdot\frac{3\pi}{4}\right)}; \\ t \mod T_{sub} & \in & \left[\frac{i\cdot T_{sub}}{8}, \frac{(i+1)\cdot T_s}{8}\right], \end{cases} \quad (17)$$

with $i \in [0,1,2,3,4,5,6,7]$. Note from [17] that most of the energy of $SC_{P,8,SSB}(t)$ and $SC^*_{P,8,SSB}(t)$ is located in the fundamental harmonics, F_{sub} and $-F_{sub}$, respectively. On the other hand, the energy of $SC_{P,8,SSB}(t)$ and $SC^*_{P,8,SSB}(t)$ is located in the harmonics $-3F_{sub}$, $5F_{sub}$ and $3F_{sub}$, $-5F_{sub}$, respectively.

B. GNSS Meta-signal Examples

In previous works, three different GNSS meta-signals have been proposed

- Galileo E5A + E6-BC: AltBOC(50,10,5) [5], [6],
- Galileo E5B + E6-BC: AltBOC(35,10,5) [5], [6]
- GPS L5 + L2C: AltBOC(25,10,1) [6].

In both works [5], [6], the GNSS Meta-signal build from the combination of the Galileo E5b and Galileo E6-BC signals has been shown to be especially interesting. This is due to the fact that this specific GNSS meta-signal is centered at 1242.925 MHz which is exactly half frequency of the carrier frequency of a possible S-band signal [5]. In this paper, we focus on those GNSS meta-signals build from the combination of different Galileo signals. Then, in the following subsection we summarize the signal structure of Galileo E5 and Galileo E6.

B.1) Galileo E5

Within the Galileo E5 band, the Galileo System generates and broadcasts the $s_{E5}(t)$ signal. This signal is separated in four signal components and it is allocated in two different frequency sub-bands, denoted as E5-A (1176.45 MHz) and E5-B (1207.14 MHz). Within each sub-band, one data component (in-phase), denoted as $s_{E5_{X,I}}(t)$, and one pilot component (in quadrature), denoted as $s_{E5_{X,Q}}(t)$, are transmitted. Note that X denotes the frequency sub-band, yielding to $X = A$ when the frequency sub-band is E5-A and $X = B$ when the frequency sub-band is E5-B [20].

The signal components contain the following elements:

- The F/NAV navigation message [20] $d_{E5_{A,I}}(t)$, transmitted by the signal component $s_{E5_{A,I}}(t)$ with a symbol rate of 50 symbols/s.
- The I/NAV navigation message [20] $d_{E5_{B,I}}(t)$, transmitted by the signal component $s_{E5_{B,I}}(t)$ with a symbol rate of 250 symbols/s.
- The ranging code $c_{E5_{A,I}}(t)$, transmitted by the signal component $s_{E5_{A,I}}(t)$, is a tiered code, where a secondary code sequence of length 20 symbols is used to modify successive repetitions of a primary PRN

sequence of 10230 chips. The tiered code period lasts 20 ms.

- The ranging code $c_{E5_{A,Q}}(t)$, transmitted by the signal component $s_{E5_{A,Q}}(t)$, is a tiered code, where a secondary code sequence of length 100 symbols is used to modify successive repetitions of a primary PRN sequence of 10230 chips. The tiered code period lasts 100 ms
- The ranging code $c_{E5_{B,I}}(t)$, transmitted by the signal component $s_{E5_{B,I}}(t)$, is a tiered code, where a secondary code sequence of length 4 symbols is used to modify successive repetitions of a primary PRN sequence of 10230 chips. The tiered code period lasts 4 ms
- The ranging code $c_{E5_{B,Q}}(t)$, transmitted by the signal component $s_{E5_{B,Q}}(t)$, is a tiered code, where a secondary code sequence of length 100 symbols is used to modify successive repetitions of a primary PRN sequence of 10230 chips. The tiered code period lasts 100 ms
- The central frequency of the Galileo E5 band is 1191.75 MHz.

B.2) Galileo E6

The signal transmitted in the Galileo E6 band, denoted as $s_{E6}(t)$, has two components: the data component $s_{E6-B}(t)$ which transmits the navigation message, called C/NAV message [20], and the pilot component $s_{E1-C}(t)$.

The signal components contain the following elements:

- The C/NAV navigation message $d_{E6-B}(t)$ [20], transmitted by the signal component $s_{E6-B}(t)$ with a symbol rate of 1000 symbols/s.
- The ranging code $c_{E6-B}(t)$, transmitted by the signal component $s_{E6-B}(t)$, is a memory PRN sequence of 5115 chips and it lasts 1 ms.
- The ranging code $c_{E6-C}(t)$, transmitted by the signal component $s_{E6-C}(t)$, is a memory code generated with a primary PRN sequence of 5115 chips and a secondary code of length 100. It lasts 100 ms .
- The carrier frequency used to transmit the signal in the E6 band is 1278.76 MHz.

Then, the C/NAV navigation data message $d_{E6-B}(t)$ is modulated by the ranging code $c_{E6-B}(t)$. In parallel, the pilot component ranging code $c_{E1-C}(t)$ is generated. Finally, both signal components are added and carrier modulated.

B.3) Spectral and Correlation Properties

If one wants to compute the AltBOC Power Spectral density (PSD), it is interesting to use the signal formulation introduced in [21]. According to [21], any chip within the PRN code can be seen as a number of equal-length deterministic segments with different amplitude levels (also know as Multilevel Coded Spreading (MCS) symbols). Then, the expression of the chip waveform is given by

$$p_{chip}(t) = \sum_{n=0}^{N_x-1} a_n p_{sub_{chip}}(t - n\frac{T_c}{N_x}), \tag{18}$$

where N_x is the number of equal-length segments, i.e. sub-chips, and $p_{sub_{chip}}$ represents the sub-chip shape. Note that in the GNSS framework $p_{sub_{chip}}$ is usually assumed to be rectangular. Moreover, $\frac{T_c}{N_x}$ can be also defined as the subcarrier period T_{sub}. The transmitted signal is defined as

$$c(t) = \sum_{n=-\infty}^{+\infty} c_n p_{chip}(t - nT_c), \tag{19}$$

with c_n the amplitude of the PRN code sequence. Considering that the PRN code shows ideal statistical properties, the PSD of $c(t)$ simplifies to $G_c(f) = |C(f)|/T_c$ [21],

$$G_c(f) = \frac{1}{T_c}\frac{\sin^2\left(\frac{\pi f T_c}{N_x}\right)}{(\pi f)^2}\left|\left|\sum_{n=1}^{N_x} a_n e^{-2\pi j \frac{nfT_c}{N_x}}\right|\right|^2. \tag{20}$$

where the first term defines the PSD of a Binary Phase Shift Keying (BPSK) modulation with chip rate $\frac{T_c}{N_x}$ and the second term determines the MCS modulation family,

$$G_c(f) = G_{BPSK}(f) G_{mod}(f). \tag{21}$$

Assuming that the AltBOC transmits codes with the same chip rate (symmetrical AltBOC), one can use the approach proposed in [22] in order to compute the symmetrical AltBOC PSD. Since GNSS meta-signals may be generated by non-symmetrical AltBOC waveforms (i.e. the chip rate of the upper and lower codes are not the same), we follow the approach in [6] in order to compute the GNSS meta-signals PSD. We use the notation AltBOC(p,q,w), where $F_{sub} = pf_0$ is the subcarrier frequency with $f_0 = 1.023$ MHz, $f_{c,A} = qf_0$ and $f_{c,B} = wf_0$ are the lower and upper codes chip rate, respectively. The non-symmetrical AltBOC PSD expression is therefore [6],

$$G_{AltBOC(p,q,w)}(f) = 4\begin{bmatrix} G_{BPSK,N_A}(f)G_{mod,N_A}(f) + \\ G_{BPSK,N_B}(f)G_{mod,N_B}(f) + \\ G_{BPSK,N_{\overline{A}}}(f)G_{mod,N_{\overline{A}}}(f) + \\ G_{BPSK,N_{\overline{B}}}(f)G_{mod,N_{\overline{B}}}(f) \end{bmatrix}, \tag{22}$$

where,

$$G_{BPSK,N_A}(f) = f_{c,A}\frac{sin^2\left(\frac{\pi f}{N_A f_{c,A}}\right)}{(\pi f)^2}, \tag{23}$$

$$G_{BPSK,N_B}(f) = f_{c,B}\frac{sin^2\left(\frac{\pi f}{N_B f_{c,B}}\right)}{(\pi f)^2}, \tag{24}$$

$$G_{BPSK,N_{\overline{A}}}(f) = f_{c,\overline{A}}\frac{sin^2\left(\frac{\pi f}{N_{\overline{A}} f_{c,\overline{A}}}\right)}{(\pi f)^2}, \tag{25}$$

with $G_{BPSK,N_{\overline{A}}}(f) = G_{BPSK,N_{\overline{B}}}(f)$, $N_A = 4\,(2p/q)$, $N_B = 4\,(2p/w)$, $N_{\overline{A}} = N_{\overline{B}} = 4\,(2p/LCM(q,w))$ and $f_{c,\overline{A}} = LCM(f_{c,A}, f_{c,B})$. Note that *LCM* stands for the Least

Common Multiple operation. In addition,

$$G_{mod,N_A}(f) = \left| \sum_{n=1}^{N_{sub}} a_{n_A} e^{-2\pi j \frac{nf}{N_A f_{c,A}}} \right|^2, \quad (26)$$

$$G_{mod,N_B}(f) = \left| \sum_{n=1}^{N_{sub}} a_{n_B} e^{-2\pi j \frac{nf}{N_B f_{c,B}}} \right|^2, \quad (27)$$

$$G_{mod,N_{\overline{A}}}(f) = \left| \sum_{n=1}^{N_{sub}} a_{n_{\overline{A}}} e^{-2\pi j \frac{nf}{N_{\overline{A}} f_{c,\overline{A}}}} \right|^2, \quad (28)$$

$$G_{mod,N_{\overline{B}}}(f) = \left| \sum_{n=1}^{N_{sub}} a_{n_{\overline{B}}} e^{-2\pi j \frac{nf}{N_{\overline{A}} f_{c,\overline{A}}}} \right|^2, \quad (29)$$

where a_{n_A}, a_{n_B}, $a_{n_{\overline{A}}}$ and $a_{n_{\overline{B}}}$ are the complex values derived from $SC^*_{8,SSB}(t)$, $SC_{8,SSB}(t)$, $SC^*_{P,8,SSB}(t)$ and $SC_{P,8,SSB}(t)$, respectively (refer to (16) and (17)).

Finally, in order to define the autocorrelation function in terms of the PSD, we resort to the Wiener-Khintchine theorem [23, Chapter 10], which states that the ACF and its PSD function are a Fourier transform pair defined as,

$$ACF(t) = \int_{-\frac{Br}{2}}^{\frac{Br}{2}} G_c(f) e^{-j2\pi ft} df. \quad (30)$$

with Br the receiver bandwidth. The PSD of Galileo E5/E6 signals along with the GNSS meta-signal PSD defined by the AltBOC(50,10,5) and AltBOC(35,10,5) is illustrated in Figure 1. Note from this figure that the PSD of GNSS meta-signals slightly differs from the PSD of Galileo E5/E6. This is because the AltBOC modulation adds intermodulation products (refers to (14)) in order to keep the constant envelope shape. Note also that generating those extra intermodulation products at the receiver replica is totally unnecessary since they were not generated at the transmission engine (Galileo E5 and E6 are transmitted with two independent HPA amplifiers). The corresponding ACFs are illustrated in Figure 2, which shows that ACFs of GNSS meta-signals are narrower than those obtained for Galileo E5/E6.

V. Results

In this section, we assess the closed-form CRB in (4) for five representative GNSS signals: i) 1ms of the Galileo E6B signal with PRN code of length 5115 chips, ii) 1ms of the Galileo E5B-I with PRN code of length 10230 chips iii) 1ms of the Galileo E5 AltBOC(15,10) with PRN codes of length 10230 chips, iv) the meta-signal Galileo E5B + E6-BC, AltBOC(35,10,5), with PRN codes of length 10230 and 5115 chips, and v) the meta-signal Galileo E5A + E6-BC, AltBOC(50,10,5), with PRN codes of length 10230 and 5115 chips. Also the legacy GPS L1 C/A signal is considered for comparison. Notice that the GPS L1 C/A uses a BPSK(1), Galileo E6B a BPSK(5) and Galileo E5B-I a BPSK(10). The CRB in (4) and the corresponding MLE in (6) are computed considering $\alpha = (1+j)\cdot\sqrt{SNR_{in}/2}$. The MLE is obtained from 1000 Monte Carlo runs. These results are summarized in Fig. 3, where both time-delay CRB and MLE obtained are shown for the different signals.

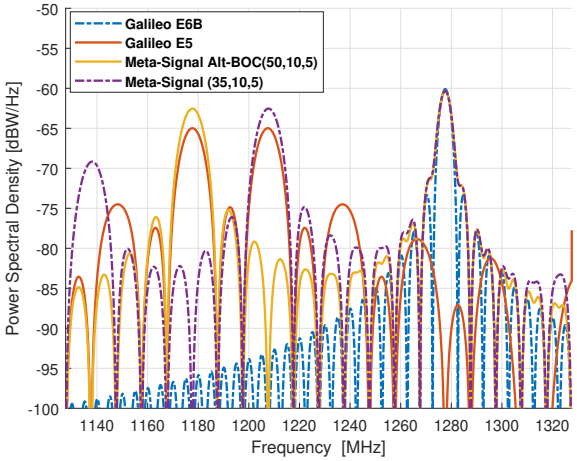

Fig. 1: Galileo E5/E6 and GNSS meta-signals PSDs

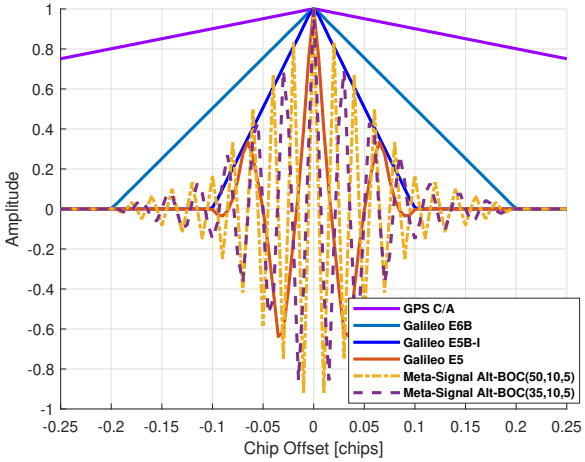

Fig. 2: GPS L1 C/A, Galileo E6B, E5B-I, E5 and GNSS meta-signals ACFs

First, note that a $\text{SNR}_{\text{out}} = 25$ dB is obtained for a $C/N_0 = 45$ dB-Hz and a coherent integration time $T_I = 10$ ms. Looking for the time-delay precision that we can obtain at this particular operation point, we obtain a standard deviation around 2.5 m for the legacy GPS L1 C/A and $F_s = 10$ MHz. Using the E6B or E5B-I signals already improves the standard GPS L1 C/A, leading to a standard deviation equal to 1 m and 63 cm, respectively, which is obvious considering the underlying BPSK(5) and BPSK(10) modulations. What is remarkable is the performance improvement provided by the Galileo E5 AltBOC(15,10) if we exploit the complete bandwidth, which at this particular operation point provides an estimate with a standard deviation equal to 8 cm. In both cases, L1, E6B, E5B-I and E5, the optimal operation threshold is around 15 dB (i.e., $C/N_0 = 35$ dB-Hz for $T_I = 10$ ms). From this value of SNR_{out} the MLE is efficient.

Considering now the results obtained with the Galileo E5B/E6B and E5A/E6 meta-signals, that is, the AltBOC(35,10,5) and AltBOC(50,10,5), respectively, and exploiting the complete bandwidth we obtain a further im-

provement. At $\text{SNR}_{\text{out}} = 25$ dB the standard deviation for the E5B/E6B is 4 cm, and for the E5A/E6 equal to 2.5 cm.

It is important to notice the behaviour of the MLE between the previous 15 dB threshold and the convergence to the CRB. This is because of the special shape of the ACF, shown in Fig. 2. With respect to the E5, these meta-signals have positive secondary ACF peaks which are very close to the main peak. These secondary peaks induce a second operation region of the MLE between the CRB and the threshold. Indeed, in this intermediate operation region the MLE jumps between secondary peaks because of the noise, which introduces estimation errors (i.e., this is the effect known as false locks in high-order BOC signals such as the BOC(15,2.5) used in the Galileo E1 PRS). We can conclude that the use meta-signals can improve the delay estimation with respect to the Galileo E5A, E5B, E6 and the complete E5 signals if the receiver is able to cope with such false locks. In addition, to reach such centimeter level accuracy the receiver needs to exploit a huge bandwidth, thus depending on the application and receiver design constraints, a wise choice may be to use the E5 AltBOC(15,10) which provides 3σ delay errors below 25 cm.

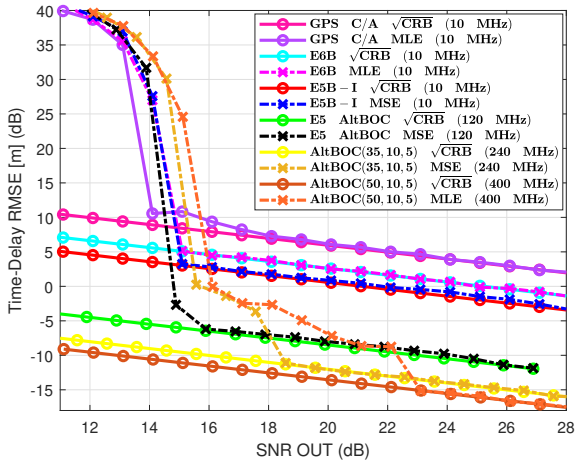

Fig. 3: CRB/MLE for GPS L1 C/A BPSK(1), E6B BPSK(5), E5B-I BPSK(10), E5 AltBOC(15,10), meta-signal E5B/E6 AltBOC(35,10,5) and meta-signal E5A/E6 AltBOC(50,10,5).

VI. Conclusions

In this article we explored the achievable delay estimation capabilities of AltBOC-type signals, either using the E5 signal or the combination of frequency bands known as GNSS meta-signal. The estimation performance is obtained with a compact closed-form CRB expression which only depends on the signal samples. It has been shown that using the E5 signal we can reduce the delay standard deviation by a factor 25, 10 and 8 with respect to the L1 C/A, E6B and E5B-I signals, respectively. This performance can be further improved by an additional factor 2 and 4 using the E5B/E6 and E5A/E6 meta-signals. The latter comes at expenses of possible false locks due to high secondary correlation peaks and a huge bandwidth. These results confirm that AltBOC-type signals can provide decimetric accuracy, thus being a promising solution for code-based precise positioning.

References

[1] M. G. Amin, P. Closas, A. Broumandan, and J. L. Volakis. Vulnerabilities, threats, and authentication in satellite-based navigation systems [scanning the issue]. *Proceedings of the IEEE*, 104(6):1169–1173, 2016.

[2] D. Medina, H. Li, J. Vilà-Valls, and Pau Closas. Robust Statistics for GNSS Positioning under Harsh Conditions: a Useful Tool? *Sensors*, 19(24), Dec. 2019.

[3] P. J. G. Teunissen and O. Montenbruck, editors. *Handbook of Global Navigation Satellite Systems*. Springer, Switzerland, 2017.

[4] H. L. Van Trees and K. L. Bell, editors. *Bayesian Bounds for Parameter Estimation and Nonlinear Filtering/Tracking*. Wiley/IEEE Press, NY, USA, 2007.

[5] J. Issler, M. Paonni, and B. Eissfeller. Toward centimetric positioning thanks to l- and s-band gnss and to meta-gnss signals. In *2010 5th ESA Workshop on Satellite Navigation Technologies and European Workshop on GNSS Signals and Signal Processing (NAVITEC)*, pages 1–8, Dec 2010.

[6] M. Paonni, J. T. Curran, M. Bavaro, and J. Fortuny. Gnss meta-signals: Coherently composite processing of multiple gnss signals. 09 2014.

[7] P. Das, J. Vilà-Valls, E. Chaumette, F. Vincent, L. Davain, and S. Bonnabel. On the accuracy limit of time-delay estimation with a band-limited signal. In *Proc. of the IEEE Intl. Conf. on Acoustics, Speech and Signal Processing (ICASSP)*, Brighton, UK, May 2019.

[8] S. J. Orfanidis. *Electromagnetic Waves and Antennas*. Rutgers University.

[9] M. I. Skolnik. *Radar Handbook*. McGraw-Hill, New York, USA, 3rd edition, 1990.

[10] H. L. Van Trees. *Detection, estimation, and modulation theory, Part III: Radar – Sonar Signal Processing and Gaussian Signals in Noise*. John Wiley & Sons, 2001.

[11] J. Chen, Y. Huang Y., and J. Benesty. Time delay estimation. In Y. Huang and J. Benesty, editors, *Audio Signal Processing for Next-Generation Multimedia Communication Systems*, chapter 8, pages 197–227. Springer, Boston, MA, USA, 2004.

[12] B. C. Levy. *Principles of Signal Detection and Parameter Estimation*. Springer, 2008.

[13] B. Ottersten, M. Viberg, P. Stoica, and A. Nehorai. Exact and large sample maximum likelihood techniques for parameter estimation and detection in array processing. In S. Haykin, J. Litva, and T. J. Shepherd, editors, *Radar Array Processing*, chapter 4, pages 99–151. Springer-Verlag, Heidelberg, 1993.

[14] T. Menni, E. Chaumette, P. Larzabal, and J.P. Barbot. New results on deterministic Cramér–Rao bounds for real and complex parameters. *IEEE Trans. on SP*, 60(3):1032–1049, March 2012.

[15] P. Stoica and A. Nehorai. Performances study of conditional and unconditional direction of arrival estimation. *IEEE Trans. on ASSP*, 38(10):1783–1795, Oct. 1990.

[16] A. Renaux, P. Forster, E. Chaumette, and P. Larzabal. On the high-SNR conditional maximum-likelihood estimator full statistical characterization. *IEEE Trans. on SP*, 54(12):4840 – 4843, Dec. 2006.

[17] L. Lestarquit, G. Artaud, and J. L. Issler. Altboc for dummies or everything you always wanted to know about altboc. In *ION GNSS*, pages 961–970, 2008.

[18] Z. Yao, F. Guo, J. Ma, and M. Lu. Orthogonality-based generalized multicarrier constant envelope multiplexing for dsss signals. *IEEE Transactions on Aerospace and Electronic Systems*, 53(4):1685–1698, Aug 2017.

[19] M. Soellner and Ph. Erhard. Comparison of awgn code tracking accuracy for alternative-boc, complex-loc and complex-boc modulation options in galileo e5-band. In *Proc. of ENC GNSS*, 2003.

[20] Galileo - open service - signal in space interface control document (os sis icd v1.3). Technical report, 2016.

[21] J. Á. Á. Rodríguez. *On Generalized Signal Waveforms for Satellite Navigation*. Universitätsbibliothek der Universität der Bundeswehr München, 2008.

[22] D. Fontanella, M. Paonni, and B. Eissfeller. A novel evil waveforms threat model for new generation gnss signals: Theoretical analysis and performance. In *2010 5th ESA NAVITEC*, pages 1–8. IEEE, 2010.

[23] A.V. Oppenheim, A.S. Willsky, and S.H. Nawab. *Signals and Systems*. Prentice-Hall signal processing series. Prentice Hall, 1997.